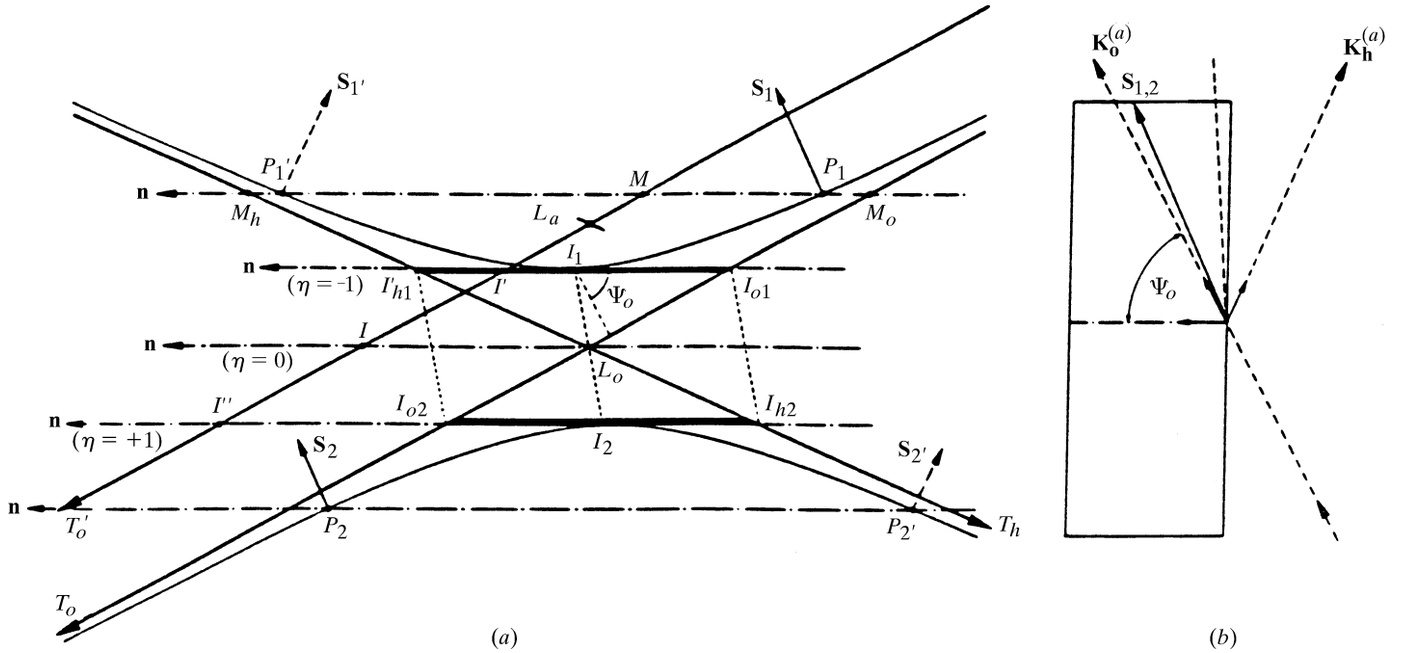


Fig. 5.1.3.5. Boundary conditions at the entrance surface for reflection geometry. (*a*) Reciprocal space; (*b*) direct space.

5.1.6.3); $\Lambda_o$ in this case is called the *Pendellösung distance*, denoted $\Lambda_L$ hereafter. Its geometrical interpretation, in the zero-absorption case, is the inverse of the diameter $A_2A_1$ of the dispersion surface in a direction defined by the cosines $\gamma_h$ and $\gamma_o$ with respect to the reflected and incident directions, respectively (Fig. 5.1.3.4). It reduces to the inverse of $A_{o2}A_{o1}$ (5.1.2.23) in the symmetric case.

In *reflection* geometry, it gives the absorption distance in the total-reflection domain and is called the *extinction* distance, denoted $\Lambda_B$ (see Section 5.1.7.1). Its geometrical interpretation in the zero-absorption case is the inverse of the length $I_{o1}I_{h1} = I_{h2}I_{o2}$, Fig. 5.1.3.5.

In a *deformed* crystal, if distortions are of the order of the width of the rocking curve over a distance $\Lambda_o$, the crystal is considered to be slightly deformed, and ray theory (Penning & Polder, 1961; Kato, 1963, 1964*a*,*b*) can be used to describe the propagation of wavefields. If the distortions are larger, new wavefields may be generated by interbranch scattering (Authier & Balibar, 1970) and generalized dynamical diffraction theory such as that developed by Takagi (1962, 1969) should be used.

Using (5.1.3.8), expressions (5.1.3.5) and (5.1.3.6) can be rewritten in the very useful form:

$$\begin{aligned}\eta &= (\Delta\theta - \Delta\theta_o)\Lambda_o \sin 2\theta/(\lambda|\gamma_h|),\\ \delta &= \lambda|\gamma_h|/(\Lambda_o \sin 2\theta).\end{aligned} \tag{5.1.3.9}$$

The order of magnitude of the Darwin width $2\delta$ ranges from a fraction of a second of an arc to ten or more seconds, and increases with increasing wavelength and increasing structure factor. For example, for the 220 reflection of silicon and Cu $K\alpha$ radiation, it is 5.2 seconds.

### 5.1.3.6. *Solution of the dynamical theory*

The coordinates of the tie points excited by the incident wave are obtained by looking for the intersection of the dispersion surface, (5.1.2.22), with the normal **Mz** to the crystal surface (Figs. 5.1.3.4 and 5.1.3.5). The ratio $\xi$ of the amplitudes of the waves of the corresponding wavefields is related to these coordinates by (5.1.2.24) and is found to be

$$\begin{aligned}\xi_j &= D_{hj}/D_{oj}\\ &= -\mathrm{S}(C)\mathrm{S}(\gamma_h)[(F_hF_{\bar h})^{1/2}/F_{\bar h}]\\ &\quad\times\left\{\eta \pm \left[\eta^2 + \mathrm{S}(\gamma_h)\right]^{1/2}\right\}/(|\gamma|)^{1/2},\end{aligned} \tag{5.1.3.10}$$

where the plus sign corresponds to a tie point on branch 1 ($j = 1$) and the minus sign to a tie point on branch 2 ($j = 2$), and $\mathrm{S}(\gamma_h)$ is the sign of $\gamma_h$ (+1 in transmission geometry, $-1$ in reflection geometry).

### 5.1.3.7. *Geometrical interpretation of the solution in the zero-absorption case*

#### 5.1.3.7.1. *Transmission geometry*

In this case (Fig. 5.1.3.4) $\mathrm{S}(\gamma_h)$ is +1 and (5.1.3.10) may be written

$$\xi_j = -\mathrm{S}(C)\left[\eta \pm (\eta^2 + 1)^{1/2}\right]/\gamma^{1/2}. \tag{5.1.3.11}$$

Let $A_1$ and $A_2$ be the intersections of the normal to the crystal surface drawn from the Lorentz point $L_o$ with the two branches of the dispersion surface (Fig. 5.1.3.4). From Sections 5.1.3.3 and 5.1.3.4, they are the tie points excited for $\eta = 0$ and correspond to the middle of the reflection domain. Let us further consider the tangents to the dispersion surface at $A_1$ and $A_2$ and let $I_{o1}$, $I_{o2}$ and $I_{h1}$, $I_{h2}$ be their intersections with $T_o$ and $T_h$, respectively. It can be shown that $\overline{I_{o1}I_{h2}}$ and $\overline{I_{o2}I_{h1}}$ intersect the dispersion surface at the tie points excited for $\eta = -1$ and $\eta = +1$, respectively, and that the *Pendellösung* distance $\Lambda_L = 1/\overline{A_2A_1}$, the width of the rocking curve $2\delta = \overline{I_{o1}I_{o2}}/k$ and the deviation parameter $\eta = \overline{M_oM_h}/\overline{A_2A_1}$, where $M_o$ and $M_h$ are the intersections of the normal to the crystal surface drawn from the extremity of any incident wavevector **OM** with $T_o$ and $T_h$, respectively.

5.1.3.7.2. *Reflection geometry*

In this case (Fig. 5.1.3.5) $S(\gamma_h)$ is now $-1$ and (5.1.3.10) may be written

$$\xi_j = S(C)\left[\eta \pm (\eta^2 - 1)^{1/2}\right]/|\gamma|^{1/2}. \qquad (5.1.3.12)$$

Now, let $I_1$ and $I_2$ be the points of the dispersion surface where the tangent is parallel to the normal to the crystal surface, and further let $I_{o1}, I_{h1}, I'$ and $I_{o2}, I_{h2}, I''$ be the intersections of these two tangents with $T_o, T_h$ and $T'_o$, respectively. For an incident wave of wavevector **OM** where $M$ lies between $I'$ and $I''$, the normal to the crystal surface drawn from $M$ has no real intersection with the dispersion surface and $\overline{I'I''}$ defines the total-reflection domain. The tie points $I_1$ and $I_2$ correspond to $\eta = -1$ and $\eta = +1$, respectively, the extinction distance $\Lambda_L = 1/\overline{I_{o1}I_{h1}}$, the width of the total-reflection domain $2\delta = \overline{I_{o1}I_{o2}}/k = \overline{I'I''}/k$ and the deviation parameter $\eta = -\overline{M_oM_h}/\overline{I_{o1}I_{h1}}$, where $M_o$ and $M_h$ are the intersections with $T_o$ and $T_h$ of the normal to the crystal surface drawn from the extremity of any incident wavevector **OM**.

### 5.1.4. Standing waves

The various waves in a wavefield are coherent and interfere. In the two-beam case, the intensity of the wavefield, using (5.1.2.14) and (5.1.2.24), is

$$|D|^2 = |D_o|^2 \exp(4\pi \mathbf{K}_{oi} \cdot \mathbf{r}) \times [1 + |\xi|^2 + 2C|\xi| \cos 2\pi(\mathbf{h} \cdot \mathbf{r} + \Psi)], \qquad (5.1.4.1)$$

where $\Psi$ is the phase of $\xi$,

$$\xi = |\xi| \exp(i\Psi). \qquad (5.1.4.2)$$

Equation (5.1.4.1) shows that the interference between the two waves is the origin of *standing waves*. The corresponding nodes lie on planes such that $\mathbf{h} \cdot \mathbf{r}$ is a constant. These planes are therefore parallel to the diffraction planes and their periodicity is equal to $d_{hkl}$ (defined in the caption for Fig. 5.1.2.1*a*). Their position within the unit cell is given by the value of the phase $\Psi$.

In the Laue case, $\Psi$ is equal to $\pi + \varphi_h$ for branch 1 and to $\varphi_h$ for branch 2, where $\varphi_h$ is the phase of the structure factor, (5.1.2.6). This means that the *nodes* of standing waves lie on the maxima of the *hkl* Fourier component of the electron density for branch 1 while the *anti-nodes* lie on the maxima for branch 2.

In the Bragg case, $\Psi$ varies continuously from $\pi + \varphi_h$ to $\varphi_h$ as the angle of incidence is varied from the low-angle side to the high-angle side of the reflection domain by rocking the crystal. The nodes lie on the maxima of the *hkl* Fourier components of the electron density on the low-angle side of the rocking curve. As the crystal is rocked, they are progressively shifted by half a lattice spacing until the anti-nodes lie on the maxima of the electron density on the high-angle side of the rocking curve.

Standing waves are the origin of the phenomenon of anomalous absorption, which is one of the specific properties of wavefields (Section 5.1.5). Anomalous scattering is also used for the location of atoms in the unit cell at the vicinity of the crystal surface: when X-rays are absorbed, fluorescent radiation and photoelectrons are emitted. Detection of this emission for a known angular position of the crystal with respect to the rocking curve and therefore for a known value of the phase $\Psi$ enables the emitting atom within the unit cell to be located. The principle of this method is due to Batterman (1964, 1969). For reviews, see Golovchenko *et al.* (1982), Materlik & Zegenhagen (1984), Kovalchuk & Kohn (1986), Bedzyk (1988), Authier (1989), and Zegenhagen (1993).

### 5.1.5. Anomalous absorption

It was shown in Section 5.1.2.2 that the wavevectors of a given wavefield all have the same imaginary part (5.1.2.17) and therefore the same absorption coefficient $\mu$ (5.1.2.19). Borrmann (1950, 1954) showed that this coefficient is much smaller than the normal one $(\mu_o)$ for wavefields whose tie points lie on branch 1 of the dispersion surface and much larger for wavefields whose tie points lie on branch 2. The former case corresponds to the *anomalous transmission effect*, or *Borrmann effect*. As in favourable cases the minimum absorption coefficient may be as low as a few per cent of $\mu_o$, this effect is very important from both a fundamental and a practical point of view.

The physical interpretation of the Borrmann effect is to be found in the standing waves described in Section 5.1.4. When the nodes of the electric field lie on the planes corresponding to the maxima of the *hkl* component of the electron density, the wavefields are absorbed anomalously less than when there is no diffraction. Just the opposite occurs for branch 2 wavefields, whose anti-nodes lie on the maxima of the electron density and which are absorbed more than normal.

The effective absorption coefficient $\mu$ is related to the imaginary part of the wavevectors through (5.1.2.19),

$$\mu = -4\pi\gamma_o K_{oi},$$

and to the imaginary part of the ratio of the amplitude of the reflected to the incident wave through

$$\mu = \mu_o - 4\pi X_{oi}, \qquad (5.1.5.1)$$

where $X_{oi}$ is the imaginary part of $X_o$, which, using (5.1.2.24) and (5.1.3.10), is given by

$$X_o = R\lambda|C|S(\gamma_h)(F_hF_{\bar{h}})^{1/2} \times \{\eta \pm [\eta^2 + S(\gamma_h)]^{1/2}\}/\left[2\pi V(|\gamma|)^{1/2}\right]. \qquad (5.1.5.2)$$

Taking the upper sign (+) for the $\pm$ term corresponds to tie points on branch 1 and taking the lower sign $(-)$ corresponds to tie points on branch 2.

The calculation of the imaginary part $X_{oi}$ is different in the Laue and in the Bragg cases. In the former case, the imaginary part of $(\eta^2 + 1)^{1/2}$ is small and can be approximated while in the latter, the imaginary part of $(\eta^2 - 1)^{1/2}$ is large when the real part of the deviation parameter, $\eta_r$, lies between 1 and $-1$, and cannot be calculated using the same approximation.

### 5.1.6. Intensities of plane waves in transmission geometry

5.1.6.1. *Absorption coefficient*

In transmission geometry, the imaginary part of $X_o$ is small and, using a first-order approximation for the expansion of $(\eta^2 + 1)^{1/2}$, (5.1.5.1) and (5.1.5.2), the effective absorption coefficient in the absorption case is

$$\mu_j = \mu_o\left[\tfrac{1}{2}(1 + \gamma^{-1}). \mp \frac{(\eta_r/2)(1 - \gamma^{-1}) + |C|(\gamma^{-1})^{1/2}|F_{ih}/F_{io}| \cos\varphi}{(\eta_r^2 + 1)^{1/2}}\right], \qquad (5.1.6.1)$$

where $\varphi = \varphi_{rh} - \varphi_{ih}$ is the phase difference between $F_{rh}$ and $F_{ih}$ [equation (5.1.2.10)], the upper sign $(-)$ for the $\mp$ term corresponds to branch 1 and the lower sign (+) corresponds to branch 2 of the dispersion surface. In the symmetric Laue case ($\gamma = 1$, reflecting planes normal to the crystal surface), equation (5.1.6.1) reduces to



references